Observation of 4 nm Pitch Stripe Domains Formed by Exposing Graphene to Ambient Air

Daniel S. Wastl,[†,*] Florian Speck,[‡] Elisabeth Wutscher,[†] Markus Ostler,[§] Thomas Seyller,[§] and Franz J. Giessibl[†]

[†]Institut für experimentelle und angewandte Physik, Universität Regensburg, 93053 Regensburg, Germany, [‡]Lehrstuhl für Technische Physik, Universität Erlangen-Nürnberg, 91058 Erlangen, Germany, and [§]Institut für Physik, Technische Universität Chemnitz, 09126 Chemnitz, Germany

ABSTRACT We study epitaxial graphene on the 6H-SiC(0001) surface under ambient conditions using frequency-modulation atomic force microscopy. We observe large terraces with a self-assembled stripe structure within a highly adsorbate covered surface on top of the graphene. To identify the origin of the structure, we compare the experimental data on graphene with calculations and experiments on graphite that predict the formation of a solid–gas monolayer in the solid–liquid interface of hydrophobic surfaces.

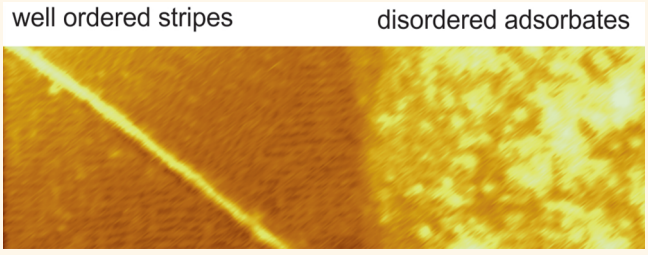

KEYWORDS: graphene · self-assembly · stripe structure · ambient environment · atomic force microscopy

Graphene is a two-dimensional crystal[1] made of carbon atoms ordered in a honeycomb lattice.[2] This material is interesting due to its properties such as high charge carrier mobility and its potential as a building block for a new generation of electronic devices. The possibilities of chemical and molecular doping of graphene and related structures,[3,4] chemical sensing, and gas detection down to the single molecular regime[5,6] have been demonstrated. High-performance sensors based on chemically derived graphene have been realized.[6–10] Graphene-based biosensors for detection of glucose,[11] bacteria,[12] pH, and proteins[13,14] have also been fabricated.

A bulk three-dimensional crystal exposes only the surface atoms to the environment, but in the case of a 2D crystal, all atoms are at the surface and are unprotected. This can easily affect the electronic transport properties[4] due to unwanted adsorbates. The preparation of a graphene flake by exfoliation[2,15] is mainly performed under ambient conditions, and the sample is exposed to air until being used. Here, surfaces stay in contact with water vapor, oxygen, nitrogen, rare gases, carbon oxides, and all other constituents of the laboratory air, including pollutants and aerosols, which can adsorb on the sample. As a result, such samples deviate from the conception of an ideal, clean graphene layer. In the future, processing of electronic devices from graphene could be an important part of modern industry. Therefore, it is important to know the surface properties and possible reactions of graphene in different environments. In this paper, we present frequency-modulation atomic force microscopy (FM-AFM)[16] measurements of epitaxial graphene on SiC(0001) in ambient conditions to clarify what happens to graphene when it is stored in air. In our data, we observed a self-assembled stripe structure, whose origin we investigate. It is proposed that the stripes mark the presence of bilayer graphene on SiC(0001) in air.

RESULTS AND DISCUSSION

Epitaxial graphene was grown by thermal decomposition of 6H-SiC(0001) under argon atmosphere[17] in a setup described elsewhere.[18] In contrast to the presence of an idealized flat and clean graphene sheet, we find that the surface consists of either areas with a high coverage of disordered adsorbates or areas with well-defined stripes, one-dimensional steps, and ridges.

Figure 1a shows a low-energy electron microscopy (LEEM) bright-field image taken at an electron energy of 3.3 eV on another

* Address correspondence to daniel.wastl@physik.uni-regensburg.de.

Received for review July 31, 2013 and accepted October 3, 2013.

Published online October 03, 2013
10.1021/nn403988y

sample prepared under identical conditions as the samples used for the AFM investigations. It exhibits mainly areas of two different intensities of the reflected electrons. Electron reflectivity spectra acquired in the portions of the dark (light) gray regions indicated by the solid (dotted) rectangles are presented in corresponding solid and dashed lines in Figure 1b. From the number of minima in the spectra, these regions can be assigned to monolayer (ML) and bilayer (BL) graphene.[19] A similar distribution of ML and BL graphene has been found in a previous study[17] of graphene obtained by atmospheric pressure graphitization at the same temperature as used for the present work. In that earlier study, BL nucleation was observed on the edge of the upper terraces[17] next to substrate macrosteps. In contrast, dark lines originating from substrate steps are evident within the bright regions in the micrograph in Figure 1a, showing that BL graphene formation is possible on either side of such steps on the samples discussed in this work. We attribute this to the growth conditions in the different furnaces used for graphene preparation in ref 17 and the present study.[18] It is instructive to compare the LEEM images with the sample morphology determined by AFM (Figure 2a). In Figure 2a, an AFM overview image of the epitaxial graphene surface is shown. On a large part of the surface, a high coverage of disordered adsorbates is observed. However, two very different types of areas can be distinguished, one which has a high coverage of adsorbates and another that is nearly clean. In high-resolution AFM images, such as Figure 2b, different step heights could be identified. Their typical height is 0.75 and 1.5 nm, but we also observed steps with a height of 4.5 nm in the adsorbate-free parts of the surface. These 4.5 nm substrate steps and higher ones (macrosteps) are expected in the case of ideal graphene growth due to step bunching of SiC.[17]

Based on the structural similarities of the LEEM and AFM images, the location of the ML and BL regions with respect to the substrate steps, and their relative coverage of the surface, we assign the areas covered with disordered adsorbates in the AFM images to ML graphene and the smooth parts to BL graphene. Substrate-induced charges and corrugation have been discussed to influence the reactivity of graphene.[20−24] In general, a higher reactivity of ML graphene compared to thicker graphene has been observed in oxidation[20,21] and electron transfer chemistry experiments.[22] ML graphene has been found to have a 10-fold higher chemical reactivity compared to few-layer (FL) graphene in certain cases.[22] It is known from scanning tunneling microscopy data that ML graphene has a larger corrugation compared to BL epitaxial graphene on SiC(0001).[25,26] This higher corrugation of ML graphene could induce a higher reactivity,[24,27] leading to an enhanced nucleation of adsorbates. This is an additional indication that the highly adsorbate covered region is monolayer graphene and the smooth parts of the surface are BL graphene. The observation of graphene

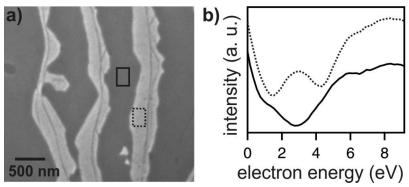

Figure 1. (a) LEEM bright-field image of epitaxial graphene prepared under the same conditions as the samples for AFM measurements. The electron energy was 3.3 eV. Regions in dark gray correspond to ML graphene and light gray to BL graphene, as evidenced by the corresponding electron reflectivity spectra shown as solid and dotted curves in (b). The spectra are offset vertically for clarity. Note the substrate steps dissecting the BL regions which appear as dark lines in the micrograph.

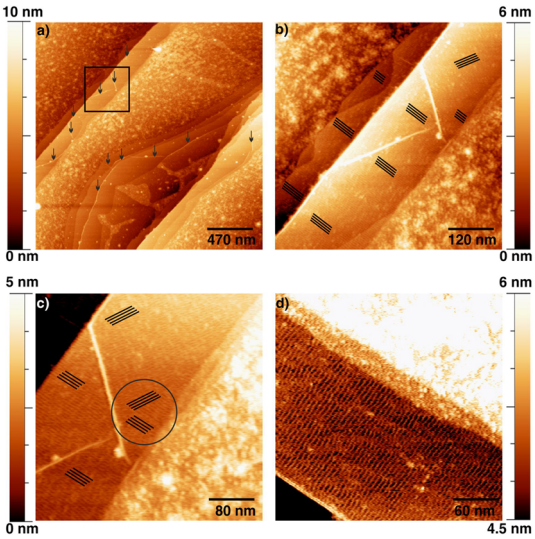

Figure 2. Epitaxially grown graphene at ambient conditions. (a) Large-scale overview with areas of high and low adsorbate density. Arrows mark ridges presumably caused by buckling and bending to relieve compressive strain. (b) Enlarged view (area marked by black box in (a)) of graphene ridges on top of the terrace. The two ridges first follow the step edge and then bend toward the center of the terrace. (c) Crossing point of the ridges. A stripe pattern on top of graphene is resolved. The orientation of the stripes in the domains is marked by solid lines and is rotated by 60° with respect to each other. The circle marks an area with mixing of domains on a terrace where the domains are not separated by a ridge. (d) High-resolution image of the sharp border between high and low adsorbate densities. The height of the striped structure is ≈0.3−0.4 nm with a periodicity of 4.2 ± 0.4 nm. Scan parameters: silicon tip (microfabricated silicon cantilever probe model Sicona, APPNANO, Santa Clara, CA, USA) attached to a qPlus[31−34] sensor, Δf = 5.04 Hz, A = 200 pm, f_0 = 25354 Hz, k = 1800 N/m, Q = 1000.

ridges[28−30] at step edges and on terraces, marked by arrows in Figure 2a, support the hypothesis that the smooth part of the surface is formed by BL graphene. The ridges are bulged regions of graphene, presumably occurring as a result of buckling and bending to relieve the compressive strain on FL graphene.[28] A typical height of 1−2 nm is found. The origin of the compressive strain is the difference between the coefficient of thermal expansion for graphene and SiC as the samples are cooled after graphitization.[29,30]

Figure 2b shows in more detail the strong separation between areas of smooth and rough surface with steps and ridges acting as borders. From high-resolution images (Figure 2c,d), one can observe that the surface is not atomically flat. Even on flat terraces, we could not get atomically resolved images of graphene. We do, however, observe a highly ordered self-assembled stripe structure.

The spacing (average periodicity extracted from 100 line-scans of 8 data sets) of these stripes is 4.2 ± 0.4 nm, and the height of the structure is 0.3−0.4 nm. This can be observed on different epitaxial graphene samples with different microscopes and tip materials.

The primary direction of the stripes is indicated by solid lines in Figure 2b,c. The stripes seem to arrange in domains, in regions where ridges are present. Related to the points discussed before, stripe domains are only present on BL or FL layer graphene. Our hypothesis to explain why we do not observe the stripe pattern on the ML graphene part is the high adsorbate coverage of ML graphene (this will be discussed later). The primary stripe domain orientation on BL graphene does not change from one terrace to the other (see Figure 2b and Figure 3). This is consistent with the observation that the graphene layer extends over substrate steps like a carpet,[25,35] a property that has been exploited in the continuous growth of molecular layers on epitaxial graphene.[36,37] Figure 2c shows two different orientations on one terrace where the orientation is marked by solid black lines in the image. The orientation of stripes in one domain is at an angle of 60° to the other. The area marked by a circle in Figure 2c shows the coexistence of different stripe orientations on one terrace.

In Figure 3, the different possible observable features of the graphene sample under ambient conditions are shown. Three kinds of surface areas labeled A, B, and C are displayed. Regions A and B are BL graphene parts of the surface, whereas part C with the high adsorbate coverage is ML graphene. The part marked by A shows only one orientation of the stripes; therefore, this whole region can be considered as one domain. Here it is clearly visible that the stripes continue over substrate steps and ridges, indicating that the BL graphene continues over step edges. Part B shows a surface area where no stripe pattern has formed on the BL graphene. This observation is rare, and it is not clear why the stripe structure is not continuous in the border region B and does not cover the complete part of the BL graphene. However, the difference between BL graphene in region B with the lower adsorbate concentration and the ML graphene assigned to part C is clearly visible. In the following, we try to clarify the origin of the observed stripe structure on BL graphene.

One possibility to create ripples in graphene could be the effect of strain in the graphene/SiC system. Duan *et al.* developed a continuum model of a graphene sheet

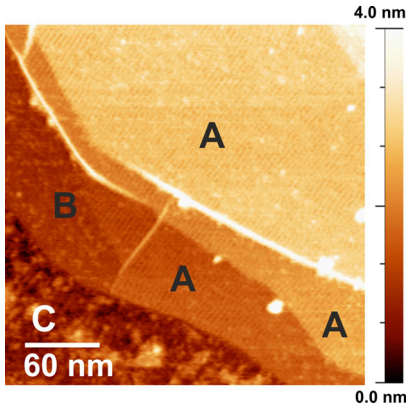

Figure 3. Epitaxially grown graphene imaged in ambient conditions: Regions A and B show BL graphene. (A) Completely covered with a stripe pattern. The stripes are continuous over substrate steps and ridges therefore region A can be treated as one large domain. (B) BL graphene with a low density of adsorbates. (C) ML graphene highly covered with adsorbates. The difference between BL graphene in B and ML graphene in C is obvious due to the higher density of disordered adsorbates. Scan parameters: silicon tip (microfabricated silicon cantilever probe model Sicona, APPNANO, Santa Clara, CA, USA) attached to a qPlus sensor, $\Delta f = 5.04$ Hz, $A = 200$ pm, $f_0 = 25354$ Hz, $Q = 1000$.

and showed that shear stress leads to the formation of wrinkles with a size- and strain-dependent amplitude and wavelength.[38] The large ridges we observe on various positions are explained by the reduction of strain in the graphene sheet.[28−30] Related to the continuum model, this strain can lead to a wrinkling of the graphene. The simulations of Duan *et al.* have shown a direct correlation between induced stress and periodicity of stripes.[38] Applying low stress to a graphene surface region induces wrinkles with a large distance between each other and therefore a low periodicity. Increasing the stress in the surface increases the periodicity of wrinkles in the simulation.[38] One would therefore expect to observe a change of the stripe direction, periodicity, and amplitude of the stripes over step edges or an orientation dependence of the domains with respect to the ridges due to the change of the strain in the surface. Experimentally, a variation of stress should be present at step edges and near ridges in the surface, as ridges are a clear indication for compensation of surface stress in graphene.[28−30] In Figure 2b, it is shown that there is no clear domain orientation dependence to the ridges or step edges and the observed periodicity and amplitude of stripes is not related to surface features. The stripe periodicity and amplitude is neither changed near ridges nor over surface steps as demonstrated in Figure 3. Also, the coexistence or mixing of domains labeled by the circle in Figure 2c excludes wrinkling of the graphene due to compressive strain as an origin for the observed stripe pattern because there should not be a spontaneous change in the surface stress on the terrace.

So far, it has not been taken into account that there is a water layer during experiments under ambient conditions. Our experiments were conducted at a

relative humidity of 50−60%. We expect that the surface is covered with an ultrathin water layer, which is present on almost all surfaces (hydrophobic or hydrophilic) exposed to air.[39,40] The thickness of the water layers adsorbed on sample surfaces depends on the relative humidity of the air,[34,41−44] and the hydrophobicity of the surface.[43,44]

In the case of water in equilibrium with air, the concentrations of dissolved oxygen and nitrogen are about 0.5 and 0.2 mM, respectively, corresponding to a molar fraction of 10×10^{-6} and 5×10^{-6}, treating air as 21% oxygen and 79% nitrogen and ignoring its other minor species.[46,45]

A numerical study of a system similar to our experimental one predicted that there might be a dramatic increase of density of gas molecules in the vicinity of a hydrophobic wall, and that they will adsorb at the liquid−solid interface[47] of hydrophobic materials. The basis of this prediction is a molecular dynamics simulation with Lennard-Jones interactions. In this previous work, it was shown that gas enrichment at hydrophobic walls is possible also when the dissolved gas concentration is very low in the bulk liquid.[47] Recently, Lu *et al.* reported the observation of a molecular layer of gas-like domains at the hydrophobic water interface on highly oriented pyrolytic graphite (HOPG) by FM-AFM.[45] After immersing the sample in water in a liquid cell which was in contact with air, they found a stripe pattern developing on the HOPG. To identify the origin of their stripe structure, they also investigated the effect of the individual components of air (N_2, O_2, CO_2, and Ar) in a closed environment liquid cell AFM chamber filled with deionized water. Their extensive studies involved different water sources, cantilevers, and microscopes to clarify the origin of the stripe structures and to exclude contaminations. They came to the conclusion that the stripes were formed by nitrogen due to a water-activated aggregation process on the hydrophobic HOPG surface.[45]

To compare the theoretical model of ref 47 and the experimental data of ref 45 to our experimental observation, we have to clarify if graphene on SiC(0001) is hydrophobic or not. HOPG is built up by stacking graphene sheets, forming a three-dimensional crystal, with a hydrophobic surface, as demonstrated by contact angle measurements.[48−50] Here the question arises if graphene on different bulk substrates has the same hydrophobic character as HOPG or a hydrophilic one. Rafiee *et al.* reported about the wetting transparency of graphene on some substrates, which means that the substrate underneath the graphene determines the wetting properties in these cases.[52] The hydrophobicity as measured by the water contact angle was found to increase with the number of graphene layers placed on the substrates.[52] Shih *et al.* showed that ML graphene is only partially transparent to the wetting property of the substrate with significant deviation from perfect transparency for superhydrophilic and superhydrophobic substrates.[53] They pointed out that, in the case of more than one graphene layer, additional screening of the influence of the substrate further reduces the wetting transparency.[53]

However, Wang *et al.* have reported a hydrophobic character for exfoliated graphene, deposited on a silicon substrate.[50] Shin *et al.* and Zhou *et al.* also reported a hydrophobic characteristic for epitaxial graphene on 6H-SiC(0001).[49,51] In particular, Shin *et al.* reported that single-, bi-, and few-layer graphene on 6H-SiC(0001) is hydrophobic with a contact angle of ≈92°.

With the knowledge of the hydrophobic character of our samples, we can compare our experimental data on graphene with the reported data of Lu *et al.*[45] on HOPG. The observed nitrogen stripe structure on HOPG is similar in periodicity and height to our findings on epitaxial graphene, but the domain size in their case is very small.[45] In our experiments, we see domains with a size of hundreds of nanometers where complete terraces are covered by the adsorbed gas and no large defects are observable (Figure 2c,d and Figure 3).

Due to the similarity to the stripes on HOPG, we propose that we also observe a solid-state gas layer on the graphene sheet. This is in agreement with the monomolecular gas layer that the numerical simulation predicted. The water in the air opens the possibility that a wetting layer forms on the surface. This wetting layer introduces the opportunity for an enrichment of gas between the solid−liquid interface, as the theoretical approach shows. Drawing from the aforementioned work of Lu *et al.* on HOPG, we propose that a condensation of N_2 molecules (gas) leads to the formation of the predicted self-assembled molecular layer related to the observed stripe structure.

We observe the same three-fold stripe domain symmetry for epitaxial graphene on SiC(0001) as for HOPG.[45] Additionally, it should be mentioned that we only observe the stripe pattern on few-layer graphene in our experiments.

ML graphene is highly covered with disordered adsorbates, which precludes the formation of an ordered stripe structure resulting from gas enrichment at the graphene−water interface. On BL graphene, however, an ordered adsorbate layer resembling the stripe structure reported for HOPG[45] is observed, which shows only a small contamination with additional adsorbates. This is indicative of a reduced influence of the SiC substrate or, more specifically, its interface layer to graphene, in the case of BL graphene as compared to ML graphene. We propose a formation of the stripe structure also on ML graphene when disordered adsorbates are absent. This could be possible in the case of hydrogen intercalated graphene on SiC(0001),[54] which is devoid of the peculiar interface layer present in the case of regular epitaxial graphene on that surface.[54]

CONCLUSION

We have shown different surface features on epitaxial graphene in ambient conditions. Most of the surface can be divided into either areas covered with disordered adsorbates, which we assigned to ML graphene, or areas with well-defined stripes that arise on BL graphene. We propose that these stripes are a solid monolayer of aggregated gas molecules from air, on the hydrophobic surface of epitaxial graphene on 6H-SiC(0001). This behavior was predicted by theory.[47] The stripe structure we found is similar to observations of nitrogen nucleation domains on HOPG,[45] in terms of the height and spacing of the stripes, and the orientation of the stripes registers with the hexagonal surface layer. We observed that the BL graphene on SiC(0001) without stripe structures is covered by fewer adsorbates in comparison to ML graphene. Due to the occurrence of the stripes only on BL graphene, they could serve as a marker for BL graphene on SiC(0001) under ambient conditions.

MATERIALS AND METHODS

Epitaxial graphene was grown by thermal decomposition of 6H-SiC(0001) under argon atmosphere[17] in a setup described elsewhere.[18] No special treatment was applied to the epitaxial grown graphene before scanning in laboratory air. AFM experiments were carried out with a home-built microscope operated by a Nanonis OC4 control electronic (SPECS Zurich GmbH, Switzerland). AFM images where acquired with a qPlus sensor, where a silicon tip extracted from a microfabricated silicon cantilever (probe model Sicona, APPNANO, Santa Clara, CA, USA) was attached to the free prong. Images were processed with the WSXM software.[55] LEEM measurements were carried out using a SPECS FE-LEEM P90 system under ultrahigh vacuum conditions (base pressure 2×10^{-10} mbar) after thoroughly degassing the sample at a temperature of about 600 °C. Bright-field images were taken at electron energy steps of 0.2 eV. This allows the extraction of reflectivity spectra by averaging the intensity of the reflected electrons over chosen areas.

Conflict of Interest: The authors declare no competing financial interest.

Acknowledgment. Thanks to Alfred J. Weymouth and Thomas Hofmann for discussions. We also like to thank Ferdinand Huber for discussions about preamplifiers, and Anja Merkel for technical support. Financial support from the Deutsche Forschungsgemeinschaft (GRK 1570, SFB 689, SPP1459) is kindly acknowledged.

REFERENCES AND NOTES

1. Novoselov, K. S.; Jiang, D.; Schedin, F.; Booth, T. J.; Khotkevich, V. V.; Morozov, S. V.; Geim, A. K. Two-Dimensional Atomic Crystals. *Proc. Natl. Acad. Sci. U.S.A.* **2005**, *102*, 10451–10453.
2. Geim, A. K.; Novoselov, K. S. The Rise of Graphene. *Nat. Mater.* **2007**, *6*, 183–191.
3. Wehling, T. O.; Novoselov, K. S.; Morozov, S. V.; Vdovin, E. E.; Katsnelson, M. I.; Geim, A. K.; Lichtenstein, A. I. Molecular Doping of Graphene. *Nano Lett.* **2008**, *8*, 173–177.
4. Liu, H.; Liu, Y.; Zhu, D. Chemical Doping of Graphene. *J. Mater. Chem.* **2011**, *21*, 3335–3345.
5. Schedin, F.; Geim, A. K.; Morozov, S. V.; Hill, E. W.; Blake, P.; Katsnelson, M. I.; Novoselov, K. S. Detection of Individual Gas Molecules Adsorbed on Graphene. *Nat. Mater.* **2007**, *6*, 652–655.
6. Fowler, J. D.; Allen, M. J.; Tung, V. C.; Yang, Y.; Kaner, R. B.; Weiller, B. H. Practical Chemical Sensors from Chemically Derived Graphene. *ACS Nano* **2009**, *3*, 301–306.
7. Sundaram, R. S.; Gomez-Navarro, C.; Balasubramanian, K.; Burghard, M.; Kern, K. Electrochemical Modification of Graphene. *Adv. Mater.* **2008**, *20*, 3050–3053.
8. Robinson, J. T.; Perkins, F. K.; Snow, E. S.; Wei, Z. Q.; Sheehan, P. E. Reduced Graphene Oxide Molecular Sensors. *Nano Lett.* **2008**, *8*, 3137–3140.
9. Lu, G. H.; Ocola, L. E.; Chen, J. H. Reduced Graphene Oxide for Room-Temperature Gas Sensors. *Nanotechnology* **2009**, *20*, 445502-1–445502-9.
10. Lu, G. H.; Ocola, L. E.; Chen, J. H. Gas Detection Using Low-Temperature Reduced Graphene Oxide Sheets. *Appl. Phys. Lett.* **2009**, *94*, 083111-1–083111-3.
11. Wang, Y.; Shao, Y. Y.; Matson, D. W.; Li, J. H.; Lin, Y. H. Nitrogen-Doped Graphene and Its Application in Electrochemical Biosensing. *ACS Nano* **2010**, *4*, 1790–1798.
12. Mohanty, N.; Berry, V. Graphene-Based Single-Bacterium Resolution Biodevice and DNA Transistor: Interfacing Graphene Derivatives with Nanoscale and Microscale Biocomponents. *Nano Lett.* **2008**, *8*, 4469–4476.
13. Ang, P. K.; Chen, W.; Wee, A. T. S.; Lho, K. P. Solution-Gated Epitaxial Graphene as pH Sensor. *J. Am. Chem. Soc.* **2008**, *130*, 14392–14393.
14. Ohno, Y.; Maehashi, K.; Yamashiro, Y.; Matsumoto, K. Electrolyte-Gated Graphene Field-Effect Transistors for Detecting pH and Protein Adsorption. *Nano Lett.* **2009**, *9*, 3318–3322.
15. Novoselov, K. S.; Geim, A. K.; Morozov, S. V.; Jiang, D.; Zhang, Y.; Dubonos, S. V.; Grigorieva, I. V.; Firsov, A. A. Electric Field Effect in Atomically Thin Carbon Films. *Science* **2004**, *306*, 666–669.
16. Albrecht, T. R.; Grütter, P.; Horne, D.; Rugar, B. H. Frequency Modulation Detection Using High-Q Cantilevers for Enhanced Force Microscope Sensitivity. *J. Appl. Phys.* **1991**, *69*, 668–673.
17. Emtsev, K. V.; Bostwick, A.; Horn, K.; Jobst, J.; Kellogg, G. L.; Ley, L.; McChesney, J. L.; Ohta, T.; Reshanov, S. A.; Röhrl, J.; *et al.* Towards Wafer-Size Graphene Layers by Atmospheric Pressure Graphitization of Silicon Carbide. *Nat. Mater.* **2009**, *8*, 203–207.
18. Ostler, M.; Speck, F.; Gick, M.; Seyller, Th. Automated Preparation of High-Quality Epitaxial Graphene on 6H-SiC(0001). *Phys. Status Solidi B* **2010**, *247*, 2924–2926.
19. Hibino, H.; Kageshima, H.; Maeda, F.; Nagase, M.; Kobayashi, Y.; Yamaguchi, H. Microscopic Thickness Determination of Thin Graphite Films Formed on SiC from Quantized Oscillation in Reflectivity of Low-Energy Electrons. *Phys. Rev. B* **2008**, *77*, 075413-1–075413-7.
20. Liu, L.; Ryu, S.; Tomasik, M. R.; Stolyarova, E.; Jung, N.; Hybertsen, M. S.; Steigerwald, M. L.; Brus, L. E.; Flynn, G. W. Graphene Oxidation: Thickness-Dependent Etching and Strong Chemical Doping. *Nano Lett.* **2008**, *8*, 1965–1970.
21. Yamamoto, M.; Einstein, T. L.; Fuhrer, M. S.; Cullen, W. G. Charge Inhomogeneity Determines Oxidative Reactivity of Graphene on Substrates. *ACS Nano* **2012**, *6*, 8335–8341.
22. Sharma, R.; Baik, J. H.; Perera, C. J.; Strano, M. S. Anomalously Large Reactivity of Single Graphene Layers and Edges toward Electron Transfer Chemistries. *Nano Lett.* **2010**, *10*, 398–405.
23. Wang, Q. H.; Jin, Z.; Kim, K. K.; Hilmer, A. J.; Paulus, G. L. C.; Shih, C.-J.; Ham, M.-H.; Kim, K. K.; Sanchez-Yamagishi, J. D.; Watanabe, K.; *et al.* Understanding and Controlling the Substrate Effect on Graphene Electron-Transfer Chemistry *via* Reactivity Imprint Lithography. *Nat. Chem.* **2012**, *4*, 724–732.
24. Fan, Q. H.; Nouchi, Z.; Tanigaki, K. K. Effect of Charge Puddles and Ripples on the Chemical Reactivity of Single Layer Graphene Supported by SiO_2/Si Substrate. *J. Phys. Chem. C* **2011**, *115*, 12960–12964.

25. Lauffer, P.; Emtsev, K. V.; Graupner, R.; Seyller, Th.; Ley, L.; Reshanov, S. A.; Weber, H. B. Atomic and Electronic Structure of Few-Layer Graphene on SiC(0001) Studied with Scanning Tunneling Microscopy and Spectroscopy. *Phys. Rev. B* **2008**, *77*, 155426-1–155426-10.
26. Mallet, P.; Varchon, F.; Naud, C.; Magaud, L.; Berger, C.; Veuillen, J.-Y. Electron States of Mono- and Bilayer Graphene on SiC Probed by Scanning-Tunneling Microscopy. *Phys. Rev. B* **2007**, *76*, 041403-1–041403-4.
27. Speck, F.; Ostler, M.; Röhrl, J.; Emtsev, K. V.; Hundhausen, M.; Ley, L.; Seyller, Th. Atomic Layer Deposited Aluminum Oxide Films on Graphite and Graphene Studied by XPS and AFM. *Phys. Status Solidi C* **2010**, *7*, 398–401.
28. Sun, G. F.; Jia, J. F.; Xue, Q. K.; Li, L. Atomic-Scale Imaging and Manipulation of Ridges on Epitaxial Graphene on 6H-SiC(0001). *Nanotechnology* **2009**, *20*, 355701-1–355701-4.
29. Hass, J.; de Heer, W. A.; Conrad, E. H. The Growth and Morphology of Epitaxial Multilayer Graphene. *J. Phys.: Condens. Matter* **2008**, *20*, 323202-1–3232022-7.
30. Biedermann, L. B.; Bolen, M. L.; Capano, M. A.; Zemlyanov, D.; Reifenberger, R. G. Insights into Few-Layer Epitaxial Graphene Growth on 4H-SiC(0001) Substrates from STM Studies. *Phys. Rev. B* **2009**, *79*, 125411-1–125411-10.
31. Giessibl, F. J. High-Speed Force Sensor for Force Microscopy and Profilometry Utilizing a Quartz Tuning Fork. *Appl. Phys. Lett.* **1998**, *73*, 3956–3958.
32. Giessibl, F. J. Atomic Resolution on Si(111)-(7 × 7) by Noncontact Atomic Force Microscopy with a Force Sensor Based on a Quartz Tuning Fork. *Appl. Phys. Lett.* **2000**, *76*, 1470–1472.
33. Giessibl, F. J.; Pielmeier, F.; Eguchi, T.; An, T.; Hasegawa, Y. Comparison of Force Sensors for Atomic Force Microscopy Based on Quartz Tuning Forks and Length-Extensional Resonators. *Phys. Rev. B* **2011**, *84*, 125409-1–1254091-5.
34. Wastl, D. S.; Weymouth, A. J.; Giessibl, F. J. Optimizing Atomic Resolution of Force Microscopy in Ambient Conditions. *Phys. Rev. B* **2013**, *87*, 245415-1–245415-9.
35. Seyller, Th.; Emtsev, K. V.; Gao, K.; Speck, F.; Ley, L.; Tadich, A.; Broekman, L.; Riley, J. D.; Leckey, R. C. G.; Rader, O.; *et al.* Structural and Electronic Properties of Graphite Layers Grown on SiC(0001). *Surf. Sci.* **2006**, *600*, 3906–3911.
36. Wang, Q. H.; Hersam, M. C. Room-Temperature Molecular-Resolution Characterization of Self-Assembled Organic Monolayers on Epitaxial Graphene. *Nat. Chem.* **2009**, *1*, 206–211.
37. Huang, H.; Chen, W.; Gao, X.; Chen, Q.; Wee, A. T. S. Structural and Electronic Properties of PTCDA Thin Films on Epitaxial Graphene. *ACS Nano* **2009**, *3*, 3431–3436.
38. Duan, W. H.; Gong, K.; Wang, Q. Controlling the Formation of Wrinkles in a Single Layer Graphene Sheet Subjected to In-Plane Shear. *Carbon* **2011**, *49*, 3107–3112.
39. Palasantzas, G.; Svetovoy, V. P.; van Zwol, G. J. Influence of Ultrathin Water Layer on the van der Waals/Casimir Force between Gold Surfaces. *Phys. Rev. B* **2009**, *79*, 235434-1–235434-7.
40. James, M.; Darwish, T. A.; Ciampi, S.; Sylvester, S. O.; Zhang, Z.; Ng, A.; Gooding, J. J.; Hanley, T. L. Nanoscale Condensation of Water on Self-Assembled Monolayers. *Soft Matter* **2011**, *7*, 5309–5318.
41. Davy, S.; Spajer, M.; Courjon, D. Influence of the Water Layer on the Shear Force Damping in Near-Field Microscopy. *Appl. Phys. Lett.* **1998**, *73*, 2594–2596.
42. Wei, P. K.; Fann, W. S. The Effect of Humidity on Probe-Sample Interactions in Near-Field Scanning Optical Microscopy. *J. Appl. Phys.* **2000**, *87*, 2561–2564.
43. Huang, F. M.; Culfaz, F.; Festy, F.; Richards, D. Effect of the Surface Water Layer on the Optical Signal in Apertureless Scanning Near Field Optical Microscopy. *Nanotechnology* **2007**, *18*, 015501-1–015501-5.
44. Freund, J.; Halbritter, J.; Hörber, J. K. H. How Dry Are Dried Samples? Water Adsorption Measured by STM. *Microsc. Res. Tech.* **1999**, *44*, 327–338.
45. Lu, Y. H.; Yang, C. W.; Hwang, I. S. Molecular Layer of Gaslike Domains at a Hydrophobic-Water Interface Observed by Frequency-Modulation Atomic Force Microscopy. *Langmuir* **2012**, *28*, 12691–12695.
46. de Nevers, N. *Physical and Chemical Equilibrium for Chemical Engineers*, 2nd ed.; John Wiley & Sons: New York, 2012.
47. Dammer, S.; Lohse, D. Gas Enrichment at Liquid–Wall Interfaces. *Phys. Rev. Lett.* **2006**, *96*, 206101-1–206101-4.
48. Zhang, Y. J.; Lu, R.; Liu, Q.; Song, Y.; Jiang, L.; Liu, Y.; Zhao, Y.; Li, T. J. Influence of Surface Hydrophobicity of Substrates on the Self-Organization of Chiral Molecule. *Thin Solid Films* **2003**, *437*, 150–154.
49. Shin, Y. J.; Wang, Y.; Huang, H.; Kalon, G.; Wee, A. T. S.; Shen, Z.; Bhatia, C. S.; Yang, H. Surface-Energy Engineering of Graphene. *Langmuir* **2010**, *26*, 3798–3802.
50. Wang, S.; Zhang, Y.; Abidi, N.; Cabrales, L. Wettability and Surface Free Energy of Graphene Films. *Langmuir* **2009**, *25*, 11078–11081.
51. Zhou, H.; Genesh, P.; Presser, V.; Wander, M. C. F.; Fenter, P.; Kent, P. R. C.; Jiang, D.; Chialov, A. A.; McDonough, J.; Shuford, K. L.; *et al.* Understanding Controls on Interfacial Wetting at Epitaxial Graphene: Experiment and Theory. *Phys. Rev. B* **2012**, *85*, 035406-1–035406-11.
52. Rafiee, J.; Mi, X.; Gullapalli, H.; Thomas, A. V.; Yavari, F.; Shi, Y.; Ajayan, P. M.; Koratkar, N. A. Wetting Transparency of Graphene. *Nat. Mater.* **2012**, *11*, 217–222.
53. Shih, C.-J.; Wang, Q. H.; Lin, S.; Park, K.-C.; Jin, Z.; Strano, M. S.; Blankstein, D. Breakdown in the Wetting Transparency of Graphene. *Phys. Rev. Lett.* **2012**, *109*, 176101-1–176101-5.
54. Riedl, C.; Coletti, C.; Iwasaki, T.; Zakharov, A. A.; Starke, U. Quasi-Free-Standing Epitaxial Graphene on SiC Obtained by Hydrogen Intercalation. *Phys. Rev. Lett.* **2009**, *103*, 246804-1–246804-4.
55. Horcas, I.; Fernandez, R.; Gomez-Rodriguez, J. M.; Colchero, J.; Gomez-Herrero, J. WSXM: A Software for Scanning Probe Microscopy and a Tool for Nanotechnology. *Rev. Sci. Instrum.* **2007**, *78*, 013705-1–013705-8.